Chapter 1

Current Status of Double Decay Experiments

1.1 Detector Design Considerations

Double beta decay experiments search for a small signal from $0\nu2\beta$ hidden amongst backgrounds from natural radioactivity and $2\nu2\beta$. Though the $0\nu2\beta$ process has not yet been observed, many $0\nu2\beta$ decay search experiments using different techniques exist, and these experiments have set ever more stringent limits of $0\nu2\beta$ and improved the half-life measurement of $2\nu2\beta$.

The expected half-life sensitivity of a $0\nu2\beta$ decay experiment can be approximately parameterised using the following equation [1]:

$$T_{1/2}^{0\nu} > \frac{4.16 \times 10^{26} yr}{n_\sigma} \left(\frac{\epsilon a}{Z}\right) \sqrt{\frac{Mt}{N_B}} \tag{1.1}$$

where

- $T_{1/2}^{0\nu}$ is the half-life sensitivity to $0\nu2\beta$ in years
- n_σ is the number of standard deviations for a given confidence level (90% CL corresponds to $n_\sigma = 1.64$)

- ϵ is the event detection and identification efficiency
- a is the isotopic abundance of the $0\nu2\beta$ source isotope in the source mass
- Z is the molecular weight of the source isotope
- Mt is the total exposure of the experiment in kg·yr
- N_B is the number of expected background events for the exposure

This equation is valid for a relatively large number of expected background events, where a Gaussian approximation of Poissonian statistics is valid, so the error is $\sqrt{N_B}$. In cases where the number of expected background events is not sufficiently high, it may still provide indications as to how experimental parameters may affect the half-life sensitivity. The equation shows that in order to maximise the half-life sensitivity in an experiment, it requires:

- a high detection efficiency
- the highest possible mass of the isotope
- the lowest possible background

Besides, to achieve a better sensitivity, it also requires the detector to have:

- good energy resolution of the detector, which helps reduce the impact of both the natural radioactivity and the $2\nu2\beta$ process high-energy tail in the Region of Interest (ROI).
- good spatial resolution to reduce the background from random coincidences.

For a zero-background experiment, the sensitivity follows

$$T_{1/2}^{0\nu} \propto \cancel{\epsilon N_{\text{atoms}} t} = \epsilon \frac{N_A a M}{Z} t \tag{1.2}$$

where N_A is Avogadro's constant. One major advantage of the zero-background experiment is that the sensitivity is proportional to the exposure Mt.

1.1.1 Isotopes

12 isotopes have been observed to undergo $2\nu2\beta$ decay, all of which are $0\nu2\beta$ decay candidates. The experimental considerations of choosing the isotope includes:

- high isotope $Q_{\beta\beta}$ value to reduce possible background from natural radioactivity
- possibility of increasing the mass of isotope, which is limited by the natural abundancy and ease of enrichment.
- high phase-space
- high NME

The list of most promising $2\nu2\beta$ decay isotopes are summarised in Table 1.1. While the majority of isotopes can be enriched via centrifugation, which is relatively low in cost for producing a large mass of the isotope, electromagnetic separation is currently the only possible method for producing ^{48}Ca, ^{96}Zr, and ^{150}Nd.

1.1.2 Radio-purity

As shown in Equation 1.1, in order to maximise the sensitivity of the experiment, the largest possible exposure is required, meaning as many atoms as possible of double beta decay isotope should be studied for the longest possible time. In addition, the best possible detector efficiency to detect the event it also required, in the case a $0\nu2\beta$ process does occur. One dominant background contribution is from the natural radioactive isotopes ^{214}Bi and ^{208}Tl, which come from ^{238}U and ^{232}Th contamination in the detector materials, hence where N_B usually increases

Isotope	$Q_{\beta\beta}$ keV	$G^{0\nu}$ $10^{-14} yr^{-1}$	NA %	Enrichment Possibilities Current Method	R&D Method(s)
^{48}Ca	4276	7.15	0.187	EMS	Laser Separation, Gaseous Diffusion
^{76}Ge	2039	0.71	7.8	Centrifugation	-
^{82}Se	2992	3.11	9.2	Centrifugation	-
^{96}Zr	3348	5.63	2.8	EMS	Laser Separation
^{100}Mo	3034	5.03	9.6	Centrifugation	-
^{116}Cd	2804	5.44	7.6	Centrifugation	-
^{130}Te	2529	4.89	34.5	Centrifugation	-
^{136}Xe	2467	5.13	8.9	Centrifugation	-
^{150}Nd	3368	23.2	5.6	EMS	Laser Separation, Centrifugation

Table 1.1: Details of isotopes commonly used in $0\nu2\beta$ experiments, showing Q-value, phase-space factor, natural abundance (NA), and possibilities for enrichment. EMS is the electromagnetic separation. $G^{0\nu}$ is calculated with $g_A = 1.25$ and $R = 1.2\ A^{1/3}$ fm [2, 3].

linearly with exposure in real-life operation, with such a dependency on exposure reduces to $\sqrt{Mt}$.

The half-life sensitivity of an experiment is given as $1/\sqrt{N_B}$. As such, the best sensitivity will be achieved by minimising the number of background events while keeping a high signal efficiency. One main background contribution is the natural radioactive isotopes ^{214}Bi and ^{208}Tl, which come from ^{238}U and ^{232}Th contamination in the detector construction materials.

To suppress the backgrounds from radioactive contamination, the detector materials must be carefully chosen to be extremely radiopure. For example, to reach a sensitivity to the Majorana neutrino mass of $10meV$ level, it is expected that materials will require radiopurity below the μ/kg level. To further reduce this contribution, it is also preferable to select an isotope with $Q_{\beta\beta} > 2.6$ MeV (as listed in Table 1.1) . This greatly reduces the background from ^{208}Tl, which has the highest energy γ-line (at 2.6 MeV) in the ^{232}Th decay chains.

1.1.3 Location

Except for contamination of the detector materials, there are external sources of background for rare event search experiments, one of which are cosmic muons. A typical $0\nu2\beta$ experiment has at least 2500 water-equivalent of rock to ensure the suppression of cosmic background, and as such it is essential to locate the experiment in an underground laboratory. Figure 1.1 shows a list of the major underground laboratories around the world.

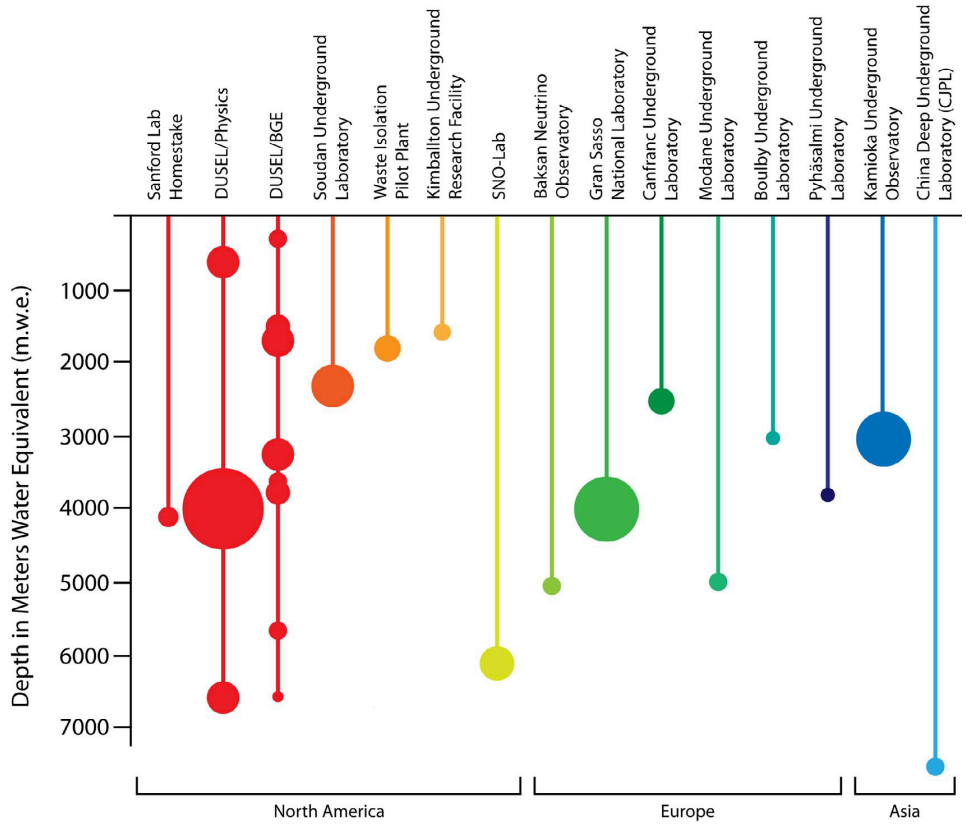

Figure 1.1: A list of the world major underground laboratories, their respective depth in meters water equivalent (m.w.e.), and their volume (represented by the size of the circles) [4].

1.1.4 Shielding

Additional shielding can provide further reduction of the background from external sources. The cosmic muon background can be suppressed further by using active shielding. As background from the surrounding environment, i.e. rocks

and materials in the lab, usually consist of gamma radiation or neutrons, radio-pure lead, ultra-pure copper, and water shielding are generally chosen to protect the detector. In addition, there is usually a detector shell made of radio-pure materials to act as a radon barrier.

One external background that can not be shielded against are the ^{8}B solar neutrinos, which increase proportionally to the detector mass. For the current experiments, like SNO+, this is already expected to be a major background.

1.1.5 Energy Resolution

In principle, the signal window of the $0\nu2\beta$ decay should be very narrow, but experimentally it is limited by the energy resolution of the detector. The excellent detector energy resolution can help to narrow down the range of signal on the total electron energy spectrum, and therefore, reduce the background. As discussed in Section **??**, the tail of $2\nu2\beta$ decay is an irreducible background to the search for $0\nu2\beta$ decay. A good energy resolution is the only practical way to suppress $2\nu2\beta$ background.

1.2 Detector Technologies of Various $0\nu2\beta$ Experiments

1.2.1 Semiconductor Experiments

In the semiconductor experiments, the $0\nu2\beta$ decay source material is usually some form of the semiconductor. When a double beta decay event occurs, the emitted electrons ionise the semiconductor, leading to a cascade of electron/hole pairs that drift to electrodes on the face of the detector, generating a voltage pulse that can be measured. As ^{76}Ge can be readily enriched to above 80% to produce large crystals which have a depletion layer of a few centimetres, allowing total absorption of gamma rays up to $\sim$ 5 MeV, it is the most popular

isotope. Germanium detectors of this size are often referred to as high-purity germanium (HPGe) detectors. The enriched HPGe detectors are the source and detector at the same time. To minimise the background, the HPGe detectors are required to be extraordinarily radio-pure.

HPGe detectors operate at cryogenic temperatures to reduce thermal noise. Also, in this configuration, they can achieve excellent energy resolution of ~ 0.15% at ^{76}Ge $Q_{\beta\beta}$, which is the primary advantage of this type of experiment. However, these experiments suffer from lots of background events from the radioactive process occurring in the detector material since they can only measure the energy spectrum of the electrons.

The modern development of Broad Energy Germanium (BEGe) detectors further improve performances such as energy resolution and background reduction, and they are now used in modern $0\nu2\beta$ decay experiments. BEGe detectors also have signal electrodes of a small size, resulting in a low capacitance, which can improve the determination of energy. The increased field near the electrode can improve the identification of the event topology to reduce backgrounds.

The modern generation of semiconductor experiments, GERDA and MAJORANA, are built on the successes of the previous Heidelberg-Moscow (H-M) [5] and IGEX experiments[6]. Moreover, the GERDA and MAJORANA collaborations recently joined together to build the next generation experiment, LEGEND, which is aiming to achieve a sensitivity of $\langle m_{\beta\beta} \rangle \sim 15$ meV[7] [8].

- **GERDA** located at the Laboratori Nazionali del Gran Sasso (LNGS).

  It consists of a large mass of germanium crystals isotopically enriched to ~ 86% in ^{76}Ge that act simultaneously as both source and detectors. The detectors are mounted in low-mass copper holders with ultra-low radioactivity and immersed directly in a 64 m^3 cryostat filled with 70 tonnes of liquid argon (LAr), which works both as a coolant and as active shielding from external backgrounds [9]. The cryostat is located inside a 590 m^3

ultra-pure water tank with 66 PMTs for the detection of Cherenkov light from cosmic muons. The result of GERDA-II set a competitive half-life limit of $T^{0\nu}_{1/2} > 8.0 \times 10^{25}$ yr [10].

- **MAJORANA** experiment uses similar technology to the previous semiconductor experiments, with the main difference being the shielding. MAJORANA deploys its HPGe detectors in a custom vacuum cryostat and uses a compact shield made with lead, oxygen-free copper, electro-formed copper, and scintillator paddles. To achieve the challenge goal of extremely low backgrounds level at 0.001 cts/(keV·kg·yr), many of the detector components were made in underground facilities to ensure they met strict radiopurity requirements. In addition, more effective shielding and pulse shape discrimination are used to reduce backgrounds.

  The Majorana Demonstrator [11] used 29.7 kg of 88%-enriched ^{76}Ge and 14.4 kg of natural p-type point-contact detectors at the Sanford Underground Research Facility (SURF). The experiment has placed a half-life limit at $T^{0\nu}_{1/2} > 8.0 \times 10^{25}$ yr, translating to $m_{\beta\beta} <$ 200 - 433 meV [12].

- **COBRA** holds five different isotopes: ^{114}Cd, ^{128}Te, ^{70}Zn, ^{130}Te, and ^{116}Cd in an array of CdZnTe (CZT), which is an intrinsic semiconductor at room temperature.

  The COBRA Demonstrator consists of a 4x4x4 array of 1 cm^3 (5.9g) detectors. With the 234.7 kg d exposure, it has set limits at $T^{0\nu}_{1/2} > 1.6 \times 10^{21}$ yr, $T^{0\nu}_{1/2} > 1.9 \times 10^{21}$ yr, $T^{0\nu}_{1/2} > 6.8 \times 10^{18}$ yr, $T^{0\nu}_{1/2} > 6.1 \times 10^{21}$ yr, $T^{0\nu}_{1/2} > 1.1 \times 10^{21}$ yr respectively [13].

  While the energy resolution of COBRA experiments are not competitive with the HPGe experiments, it has the main advantage of operating at relatively high temperature ($\sim$ 20 °C). The experiment will process using a pixelated array and improved readout, enabling the possibility of particle tracking and identification, which can significantly reduce the background level. If the background reduction can be significantly improved, the tech-

nology will be used on a 415 kg detector, aiming at a sensitivity of 50 – 70 meV [14].

1.2.2 Scintillator Experiments

In the scintillator experiment, the $0\nu2\beta$ candidate isotope is placed inside the radio-pure scintillating medium surrounded with PMTs. This design allows for the observation of light emitted by the scintillator when the decay product of the $0\nu2\beta$ isotope excites the scintillation material. Generally, scintillator experiments are relatively cheap, and they can reach a high degree of radiopurity.

Scintillator experiments can be divided into two major types based on their technology. The first type is where the $0\nu2\beta$ isotope is dissolved in a large volume of liquid scintillator. This design allows for the study of large masses of isotopes such as ^{136}Xe, ^{130}Te, or ^{150}Nd. In addition, the scintillator detectors can provide relatively good detection efficiency, good self-shielding, and low background. However, these experiments suffer from poor energy resolution. The two main experiments using this technology are the KamLAND-Zen experiment studying ^{136}Xe, and the SNO+ experiment studying ^{130}Te.

- **KamLAND-Zen** use the existing KamLAND detector which was originally built to study neutrino oscillations [15]. In the centre of the KamLAND-Zen detector, there is a transparent nylon inner balloon which is 3.08 m in diameter containing 13 tonnes of Xenon-loaded liquid scintillator. It is surrounded by 1000 tonnes of liquid scintillator contained in a 13 m diameter spherical outer balloon, which provides an active shield. Outside the outer balloon, there is a layer of 1.8 m thickness transparent buffer oil. The scintillation lights are viewed by 1,879 17-inch and 20-inch PMTs mounted on the inner surface of the 18m-diameter stainless steel spherical tank, which is surrounded by a 3200-ton water-Cherenkov detector serving as a radiation shield from the surrounding rock.

  The first phase of the KamLAND-Zen experiment (Phase I) contained ~

300 kg of ^{136}Xe and achieved an exposure of 89.5 kg·yr, reaching a half-life limit of $T^{0\nu}_{1/2} > 1.9 \times 10^{25}$ yr (90% C.L.), corresponding to $\langle m_{\beta\beta} \rangle < 160$ - 330 meV[16].

After the first phase, the liquid scintillator was purified to remove impurities. In the second phase (Phase II), ~ 340 kg of ^{136}Xe was used and a reduction of ^{110m}Ag by more than a factor of 10 was found. Phase II reached an exposure of 504 kg·yr, which is equivalent to $T^{0\nu}_{1/2} > 1.9 \times 10^{25}$ yr, corresponding to $\langle m_{\beta\beta} \rangle < 61$ - 165 meV[17].

Furthermore, due to its low background level, KamLAND-Zen can observe $2\nu2\beta$ across a wide energy range and provide strong constraints on Majoron emission decay modes[18].

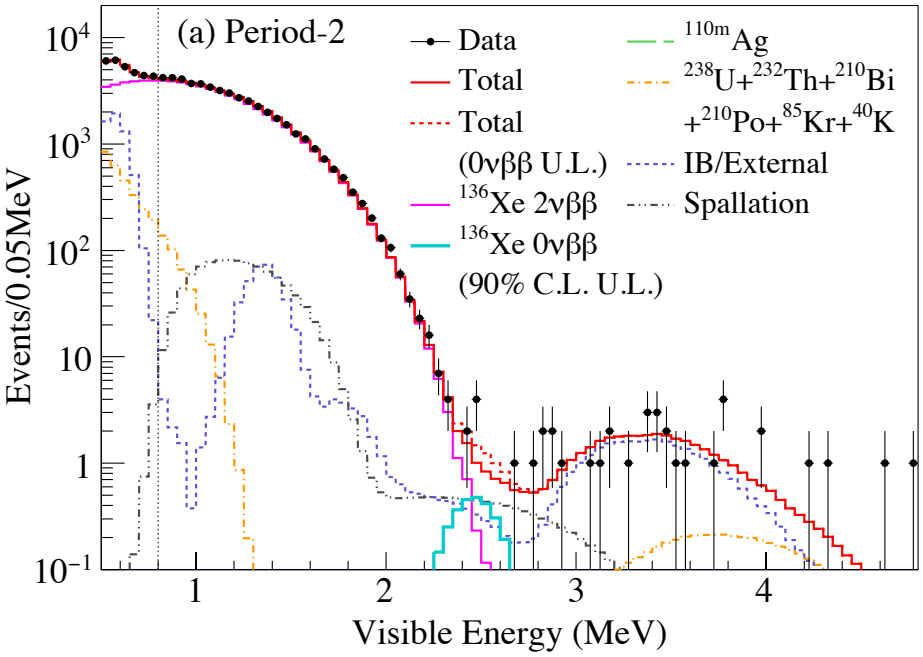

Figure 1.2: Energy spectrum showing the results from KamLAND-Zen[17].

Additionally, in a future upgrade, the KamLAND2-Zen experiment will improve the detector energy resolution as well as increase the capacity to load more isotope. Using 1 ton of ^{136}Xe, it is expected to reach $\langle m_{\beta\beta} \rangle \sim 20$ meV, fully covering the IH region[19].

- **SNO+** follows a similar principle to KamLAND-Zen but studies a different

isotope: ^{130}Te. The SNO+ detector is inherited from SNO located in the Sudbury Neutrino Observatory, which is one of the world's deepest underground laboratory (~ 6000 m.w.e.).

The detector consists of a 12 m diameter spherical acrylic vessel (AV) which is shielded by a water bath and surrounded by 9,394 8-inch PMTs mounted on a stainless steel support structure [20].

^{130}Te will be dissolved in liquid scintillator contained in a 12 m diameter acrylic sphere. This acrylic sphere is shielded by a water bath and instrumented with 9500 PMTs.

For the initial phase, ^{130}Te will be loaded at 0.3% within a scintillation solution, providing 800 kg of isotope reaching a sensitivity of $\langle m_{\beta\beta} \rangle$ < 50 - 100 meV. In the second phase, it will increase the concentration to 3%, loading 8000 kg of ^{130}Te in total, with the expected sensitivity reaching the level of $\langle m_{\beta\beta} \rangle$ <20 - 40 meV [21].

The second type of scintillator experiment is where the isotope is inherently part of the scintillator. The two most successful experiments of this type are ELEGANT VI and CANDLES III. Both of them use crystal scintillators containing ^{48}Ca.

- **ELEGANT VI** studied 23 CaF_2(Eu) crystal scintillators, which contained 7.6 g of ^{48}Ca in total. These crystals were shielded by an active veto to reduce the background. With a total exposure of 0.015 kg·yr, the ELEGANT VI experiment produced a half-life limit of $T^{0\nu}_{1/2} > 5.8 \times 10^{22}$ yr, equivalent to the $\langle m_{\beta\beta} \rangle$ < 3.5 - 22 meV [22].

- **CANDLES III** evolved from ELEGANT VI. It studies 305 CaF_2 crystals, which contain 300 g of ^{48}Ca in total. The crystals are surrounded by liquid scintillator which acts as the active shielding and removes the need for doping of the crystals. The experiment is currently taking data and is expected to achieve a sensitivity of $\langle m_{\beta\beta} \rangle$ < 50 - 100 meV of 0.5 eV. If ^{48}Ca enrichment technology can be improved in the future, the experiment can be scaled up

by an order of magnitude to study ~ 3 kg of ^{48}Ca, reaching a sensitivity of 50 meV [23].

1.2.3 Bolometer Experiments

Bolometer experiments measure the $0\nu2\beta$ through the temperature rises caused by energy absorption. When the $0\nu2\beta$ decay occurs, the emitted electrons generate heat while passing through the material, thus raising the temperature of the material by a small amount. The temperature increase is the ratio of the energy deposited over the heat capacity, and when the detector operates at a very low temperature (order of mK), the heat capacity of the material at very low temperatures T is proportional to T^3. In the bolometer experiments, the typical temperature variation is of the order of 0.1 mK per MeV of deposited energy. This temperature variation can be measured by semiconductor thermistors to determine the summed electron energy. Bolometer experiments generally have excellent energy resolution (0.3-0.5%), and high efficiency on the containment of the $0\nu2\beta$ isotopes, and can use different materials as a number of 0vbb candidates can be used grow a crystal [24]. However, this type of experiment may suffer from background because the particle identification can be challenging, and the detector response time can be long (order of seconds). Also, for the future experiments, the technical difficulty of maintaining the extremely low temperature can pose a big challenge on building larger detectors.

- **CUORE** is built on the success of the CUORICINO experiment [25] using the same technology. CUORE is composed of a tower array of 988 5Ö5Ö5cm^3 enriched and natural TeO_2 crystals working at ~ 7 mK, containing total mass of ^{130}Te to 204 kg [26]. After a short time running, the first results show CUORE has already reached a sensitivity of 1.5×10^{25} yr (90% C.L.)[26] corresponding to $\langle m_{\beta\beta}\rangle < 110$ - 520 meV.

To reduce the background, the bolometric crystal can also be used as a scintillator. By combining the temperature and scintillation light measurements,

particle identification can be improved, thus allowing for better background rejection.

- **CUPID** project will be built on the experience and skills gained from the CUORE, with upgraded Particle ID, increase mass of source and reduced background. It is aiming to achieve zero-background in the region of interest to further improve the sensitivity of $0\nu2\beta$ half-life. The two CUPID demonstrators: CUPID-0 using $Zn^{82}Se$ and CUPID-Mo using $Li_2{}^{100}100MoO_4$ have started data taking since 2017 and 2019, respectively [27] [28].

1.2.4 Time Projection Chamber Experiments

The Time Projection Chamber (TPC), which can provide a 3-dimensional reconstruction of a particle trajectory, is a popular detector technique in experimental high energy physics. There are several different designs of TPCs, but their principle remains the same. A TPC contains a sensitive gaseous or liquid medium which is embedded in the electric field. When a particle passes through, it ionises the medium and produces free electrons which drift towards a position-sensitive electron collection device. The induced current is proportional to the ionisation.

In most TPC experiments, the detector medium is also particularly selected as a scintillator, which can measure energy and provide a prompt signal for time measurement. The location of the energy deposited gives the 2-dimensional position. In addition, given the known drift speed of the free electron in a specific medium, and the measured time of arrival, it is possible to reconstruct the event in 3 dimensions. Considering the cost of enrichment, xenon is currently the most suitable medium among all double β candidate isotopes. The most promising scintillating-TPC experiments are EXO and NEXT, both of which search for $0\nu2\beta$ in ^{136}Xe, utilising the scintillating properties of xenon.

- **EXO** is located in an underground cleanroom in the WIPP. The experiment

consists of a liquid Time Projection Chamber (TPC) based on Xe. EXO-200 has completed its science run, studied 200 kg of ^{136}Xe (enriched to 80.6%). The TPC uses cylindrical geometry in order to minimise the surface and thus reduce the background contribution from the copper vessel, and it is symmetric around a central cathode plane held at a negative high voltage. At each end of the TPC, there are planes of anode wires with an array of avalanche photodiodes for ionisation and scintillation readout [29]. EXO-200 phase I started in 2011 and was interrupted in 2014, with a total exposure of 100 kg·yr. Phase II started running in 2016 with an upgraded radon suppression system and low-noise electronics, and it completed data taking in 2018. No $0\nu2\beta$ signal has been observed, thus a half-life limit has been set at $T^{0\nu}_{1/2} > 1.8\times10^{25}$ yr [30]. The EXO-200 experiment has achieved an energy resolution of 2.90% (FWHM) at $Q_{\beta\beta}$(2.458MeV for ^{136}Xe) and a background level of $1.9\pm0.2\times10^{-3}$ counts/keV/kg/y. The next generation, nEXO, will contain 5 tons of xenon enriched to 90% in ^{136}Xe, aiming for a sensitivity on the order of $10^{28}yr$. The expected energy resolution reached will be 2.90% (FWHM) with lower noise silicon photomultipliers (SiPMs) for scintillation collection [31].

- **NEXT** is a planned high-pressure gas-phase xenon TPC which is located at the Laboratorio Subterraneo de Canfranc (LSC) in Spain. Operating at high pressure (10-15 bar), the TPC can track individual particles, thus providing an effective way of rejecting background through the topological signature of events. The TPC has an asymmetric geometry, with the array of PMTs which detect both the primary scintillation light and the secondary scintillation light to reconstruct energy located at one end referred to as the energy plane, and the SiPMs used for track reconstruction located at the other end near the amplification region. The demonstrator NEXT-100 detector will contain 100 kg of xenon enriched to 91% in ^{136}Xe, aiming to achieve a background level of 0.4×10^{-3} counts/keV/kg/y and an energy resolution of < 1% (FWHM) at $Q_{\beta\beta}$ [32]. The final goal of NEXT-100 is to

reach a half life sensitivity of $T_{1/2}^{0\nu} > 2.8 \times 10^{25}$ yr after 3 years of running [32]. If the experiment is successful, the experiment will scale to contain one tonne of xenon.

1.2.5 Tracker-Calorimeter Experiments

In the tracker-calorimeter experiment, the $0\nu2\beta$ decay source is located at the centre of the detector surrounded by the tracker, followed by the calorimeter. The scattering of the emitted electrons can be minimised in the tracker, benefiting from the low-density gases. The design of tracker-calorimeter experiment allows for full reconstruction and measurement of single-particle energy. As such, the tracker-calorimeter experiments have excellent background rejection ability, and can shed light on the underlying $0\nu2\beta$ decay mechanism [33]. Tracker-calorimeter experiments perform excellently in both $2\nu2\beta$ and $0\nu2\beta$ measurements because they can achieve some of the lowest background rates among $0\nu2\beta$ experiments across the entire energy spectrum. It has been shown that the angular and electron energy difference distributions can be used to discriminate between the two prominent models, the mass mechanism (MM) and the right-handed current (RHC), as shown in Figure **??**. The separated source and detector allow for the study of different $0\nu2\beta$ isotopes. However this design suffers from relatively poor energy resolution. The most notable tracker-calorimeter experiments are the NEMO-3 and SuperNEMO experiments.

- **NEMO-3** operated from 2003 to 2011 at the Laboratoire Souterrain de Modane (LSM). It studied seven different $0\nu2\beta$ candidates, set the leading $0\nu2\beta$ decay half-life limits on four of them, and measured the most accurate $2\nu2\beta$ half-lives on all of them. The isotopes were housed in thin foils which were surrounded by the tracker containing the gas mixture of helium, argon, and alcohol, and then enclosed by a plastic scintillator calorimeter. 25G magnetic field was applied to enable charge identification. The calorimeter provided position, energy, and timing measurements of individual

particles such as electrons, positrons, γ, and α particles. The strongest limit of NEMO-3, $\langle m_{\beta\beta} \rangle < 0.3 - 0.8$ eV, is provided by 6.9 kg of ^{100}Mo with an exposure of 34.5kg·yr[34].

- **SuperNEMO** is building upon the successful NEMO-3 design, with improvements on radiopurity, calorimeter design, and detection efficiency. It will contain 20 identical modules housing 100 kg of ^{82}Se in total. The target sensitivity for SuperNEMO is $T^{0\nu}_{1/2} > 1.0 \times 10^{26}$ yr, corresponding to $\langle m_{\beta\beta} \rangle < 50 - 100$ meV[35]. The first Demonstrator Module is about to start its physics run at LSM, aiming to reach zero backgrounds in the region of interest of the $0\nu2\beta$ decay of ^{82}Se. Thanks to the tracker capabilities and segmented calorimeter, SuperNEMO is currently the only experiment which can study the underlying mechanism of $0\nu2\beta$ decay. More details of the SuperNEMO experiment can be found in Chapter **??**.

1.3 Summary of the Current and Next Generation Experiments

A wide range of experimental techniques has been applied to search for the $0\nu2\beta$ decay process. A summary of key experiments can be found in Table 1.2.

The experiments which are currently under construction or have started data-taking are sensitive to $\langle m_{\beta\beta} \rangle \sim 60$ meV, approaching the top of the region corresponding to inverted ordering of neutrino masses, and many of the next generation experiments are planning to study larger masses of $0\nu2\beta$ isotopes to achieve better sensitivity to $\langle m_{\beta\beta} \rangle \sim 10$ meV. There is a rich interplay with neutrino oscillation experiments. For example, if the inverted ordering is discovered by oscillaiton experiments the currently proposed $0\nu2\beta$ experiments should be able to observe or refute 0vbb driven by the light Majorana neutrino mass.

Experiment	Isotope	Mass (kg)	Type	Sensitivity $m_{\beta\beta}$ /meV
MAJORANA	^{76}Ge	40	Semiconductor	100 - 300
GERDA	^{76}Ge	40	Semiconductor	100 - 300
LEGEND	^{76}Ge	1000	Semiconductor	10 - 20
CUORE	^{130}Te	204	Bolometer	100 - 400
CUPID	^{100}Mo	280	Bolometer	12 - 20
KamLAND-Zen	^{136}Xe	380	Liquid Scint.	61 - 165
KamLAND2-Zen	^{136}Xe	800	Liquid Scint.	20 - 60
SNO+	^{130}Te	800	Liquid Scint.	50 - 100
EXO-200	^{136}Xe	80	Scint. TPC	190 - 450
nEXO	^{136}Xe	3700	Scint. TPC	7 - 18
NEXT-100	^{136}Xe	90	Scint. TPC	70 - 150
NEXT-HT	^{136}Xe	1000	Scint. TPC	13 - 60
NEMO-3	^{100}Mo	7	Tracker-Calo	300 - 800
SuperNEMO	^{82}Se	100	Tracker-Calo	50 - 100

Table 1.2: Summary of current and future $0\nu2\beta$ experiments.

Bibliography

[1] Frank T. Avignone, Steven R. Elliott, and Jonathan Engel. Double Beta Decay, Majorana Neutrinos, and Neutrino Mass. *Rev.Mod.Phys.*, 80:481–516, 2008.

[2] J.D. Vergados, H. Ejiri, and F. Simkovic. Theory of Neutrinoless Double Beta Decay. *Rept.Prog.Phys.*, 75:106301, 2012.

[3] Werner Rodejohann. Neutrinoless double beta decay and neutrino physics. *J.Phys.*, G39:124008, 2012.

[4] et al. A. J. LANKFORD, Y. ALHASSID. An Assessment of the Deep Underground Science and Engineering Laboratory (DUSEL). *tech. rep.*, 2011.

[5] H.V. et al. Klapdor-Kleingrothaus. Latest results from the heidelberg-moscow double beta decay experiment. *The European Physical Journal A - Hadrons and Nuclei*, 12(2):147–154, Oct 2001.

[6] C. E. et al. Aalseth. Recent results of the igex 76ge double-beta decay experiment. *Physics of Atomic Nuclei*, 63(7):1225–1228, Jul 2000.

[7] C. Cuesta et al. Background model for the majorana demonstrator. *Physics Procedia*, 61:821 – 827, 2015. 13th International Conference on Topics in Astroparticle and Underground Physics, TAUP 2013.

[8] N. et al. Abgrall.

[9] K.-H. et al. Ackermann. The gerda experiment for the search of $0\nu\beta\beta$ decay in 76ge. *The European Physical Journal C*, 73(3):2330, Mar 2013.

[10] M. et al. Agostini. Improved limit on neutrinoless double-β decay of ^{76}Ge from gerda phase ii. *Phys. Rev. Lett.*, 120:132503, Mar 2018.

[11] N. Abgrall et al. The Majorana Demonstrator Neutrinoless Double-Beta Decay Experiment. *Adv. High Energy Phys.*, 2014:365432, 2014.

[12] S. I. et al. Alvis. Search for neutrinoless double-β decay in ^{76}Ge with 26 kg yr of exposure from the majorana demonstrator. *Phys. Rev. C*, 100:025501, Aug 2019.

[13] J et al. Ebert. Results of a search for neutrinoless double-β decay using the cobra demonstrator. *Phys. Rev. C*, 94:024603, Aug 2016.

[14] Jeanne R. Wilson. Double beta decay measurement with COBRA. *Nucl.Phys.Proc.Suppl.*, 221:313–316, 2011.

[15] Junpei Shirai. Kamland-zen: Status and future. *Nuclear Physics B - Proceedings Supplements*, 237-238:28 – 30, 2013. Proceedings of the Neutrino Oscillation Workshop.

[16] A. et al. Gando. Limit on Decay of ^{136}Xe from the First Phase of KamLAND-Zen and Comparison with the Positive Claim in ^{76}Ge. *Phys.Rev.Lett.*, 110(6):062502, 2013.

[17] A. et al. Gando. Search for majorana neutrinos near the inverted mass hierarchy region with kamland-zen. *Phys. Rev. Lett.*, 117:082503, Aug 2016.

[18] A. et al. Gando. Limits on Majoron-emitting double-beta decays of ^{136}Xe in the KamLAND-Zen experiment. *Phys.Rev.*, C86:021601, 2012.

[19] A. et al. Gando. Limits on majoron-emitting double-β decays of ^{136}xe in the kamland-zen experiment. *Phys. Rev. C*, 86:021601, Aug 2012.

[20] A et al. BiaÅek. A rope-net support system for the liquid scintillator detector for the sno+ experiment. *Nuclear Instruments and Methods in Physics Research Section A Accelerators Spectrometers Detectors and Associated Equipment*, 827:152–160, 08.

[21] Jeanne R. Wilson. Non-accelerator Neutrino Physics. IoP HEPP & APP Group Meeting, 2013.

[22] S. Umehara, T. Kishimoto, I. Ogawa, R. Hazama, and H. et al. Miyawaki. Neutrino-less double-beta decay of ^{48}Ca studied by CaF_2(Eu) scintillators. *Phys.Rev.*, C78:058501, 2008.

[23] S. Umehara, T. Kishimoto, M. Nomachi, S. Yoshida, K. Matsuoka, et al. Search for neutrino-less double beta decay with CANDLES. *AIP Conf.Proc.*, 1441:448–450, 2012.

[24] Denys Poda and Andrea Giuliani. Low background techniques in bolometers for double-beta decay search. *International Journal of Modern Physics A*, 32(30):1743012, 2017.

[25] E. Andreotti, C. Arnaboldi, F.T. Avignone, M. Balata, and I. et al. Bandac. ^{130}Te Neutrinoless Double-Beta Decay with CUORICINO. *Astropart.Phys.*, 34:822–831, 2011.

[26] C. et al. Alduino. First results from cuore: A search for lepton number violation via $0\nu\beta\beta$ decay of ^{130}Te. *Phys. Rev. Lett.*, 120:132501, Mar 2018.

[27] O. et al. Azzolini. Final result of cupid-0 phase-i in the search for the ^{82}Se neutrinoless double-β decay.

[28] E. et al. Armengaud. The cupid-mo experiment for neutrinoless double-beta decay: performance and prospects. *The European Physical Journal C*, 80:44, 01 2020.

[29] J. B. et al. Albert. Searches for double beta decay of ^{134}Xe with exo-200. *Phys. Rev. D*, 96:092001, Nov 2017.

[30] J. B. et al. Albert. Search for neutrinoless double-beta decay with the upgraded exo-200 detector. *Phys. Rev. Lett.*, 120:072701, Feb 2018.

[31] et al. S. Al Kharusi. nexo pre-conceptual design report, 2018.

[32] J. et al. Martín-Albo. Sensitivity of NEXT-100 to neutrinoless double beta decay. *Journal of High Energy Physics*, 2016(5):159, May 2016.

[33] R. et al. Arnold. Probing new physics models of neutrinoless double beta decay with supernemo. *Eur.Phys.J.*, C70:927–943, 2010.

[34] L. Simard. The NEMO-3 results after completion of data taking. *J.Phys.Conf.Ser.*, 375:042011, 2012.

[35] R. Saakyan. Tracking-based Experiments in Double Beta Decay. *Nucl.Phys.Proc.Suppl.*, 229-232:135–140, 2012.